



LOCAL SCOUR AROUND SINGLE CENTRAL CIRCULAR BRIDGE PIERS LOCATED WITHIN 180° BEND

Jaafar S. Maatooq¹ and Emad S. Mahmoud²

¹Hydraulic Structures Engineering, Department of Building and Construction Engineering, University of Technology, Baghdad, Iraq

²Water Resources Engineering, Department of Building and Construction Engineering, University of Technology, Baghdad, Iraq

E-Mail: jaafarmaatooq@gmail.com

ABSTRACT

The local scour around bridge piers is one of the most common causes of bridge failures. Many equations have been proposed for determination. Most of these equations have a reliability and are used for design, were developed when the pier located within straight reaches for both flume and field studies. However, few studies have been conducted on bridge pier located within the curved channel. A laboratory work was conducted to measure the local scour which is formed around single circular pier fixed at each 30° of the bend while adopting three different diameters. The results show that the maximum depth of scour and the maximum extents (i.e., length and width) of scour hole, and maximum modification factor due to bend have occurred when the pier is located at sector 90° of the bend. The results also show that the diameter has a significant effect on scour phenomenon.

Keywords: circular pier, local scour, river bend, threshold velocity, secondary flow, clear water scour.

1. INTRODUCTION

The importance of local scour around bridge pier has been known for many years. The local scour around bridge piers is one of the most common causes of bridge failures. Scour is a natural phenomenon caused by the erosive action of the flowing water on the bed and banks of alluvial channels; thus there is a tendency to expose the foundations of a bridge pier or abutment [10]. Pier scour occurs due to a complex vortex system. This system consists of a horseshoe vortex initiated from the down flow at the upstream face of the pier, and wake vortices which shed from sides of the pier due to flow separation. This complex system digs the scour hole and deepens it [3]. Flow pattern and the mechanism of scouring around a bridge pier have been reported by various investigators. A lot of extensive experiments have been done until now to study the flow pattern and local scour. Some of the most reliable studies were carried out by; [2],[5], [10], [3], and others. All of these studies have been done in straight reaches. There is little information, to the knowledge of the authors, about the scour at bridge pier in curved channel reaches. The studies related to this context, at hand, are those conducted by; [8], [9], and [6]. The main feature of a bend flow is the presence of spiral flow, and lateral sediment transport across the channel bend is observable. Particles at the surface of the flow in the bend tend to move toward the outer wall while at the bed elevation they tend to move toward the inner wall of the channel [11]. This phenomenon of sediment movement definitely will have a direct influence on the size of scour hole and depth of scour which formed around the bridge pier when it was located within bend action.

This paper presents the experimental results of scour at a cylindrical single pier located at the centre of different sections in a 180 -degree channel bend. In order to understand the effect of bend on the scour hole, the results are compared with those in a straight channel.

2. FLOW PATTERN IN BENDS

The main feature of the flow in bends is that beside the stream wise velocity there is a secondary velocity in the radial (transverse) direction, as shown in Figure-1.

As the flow moves around a bend, the streamlines are curved, so the flow in a curved path becomes subjected to centrifugal force. Due to this centrifugal action, a pressure gradient normal to the direction of the main flow will be slightly higher near the outer bank than near the inner bank; thereby, the transverse water surface profile becomes inclined with an increase of water depth near the outer bank. Consequently, the water depth near the inner bank decreases. This difference between the water levels is called super elevation [7]. Accordingly, the faster-moving surface current will be toward the outer bank then reflected near the bed toward the inner bank (secondary current), as shown in Figure-2. This spiral action of the secondary currents are more directed on the river banks and hence cause more erosion on the concave bank (near the outer bank) and more deposition on the convex bank (near the inner bank) [14]. It should be mentioned that this action of flow within the bend reach occurs just due to the curvature feature of streamlines without taking into account the presence of other effects, such as contraction, dikes, or bridge abutments and piers.

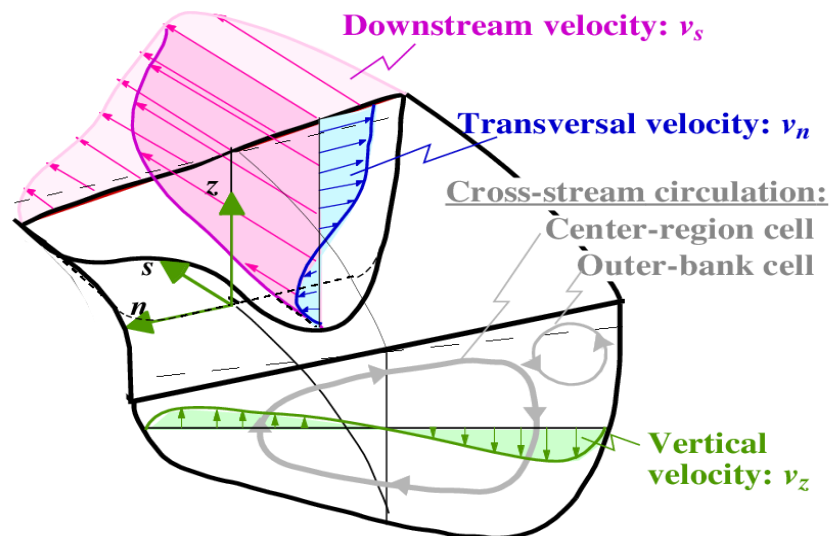


Figure-1. Transverse and longitudinal meander channel (Won and Young, 2010).

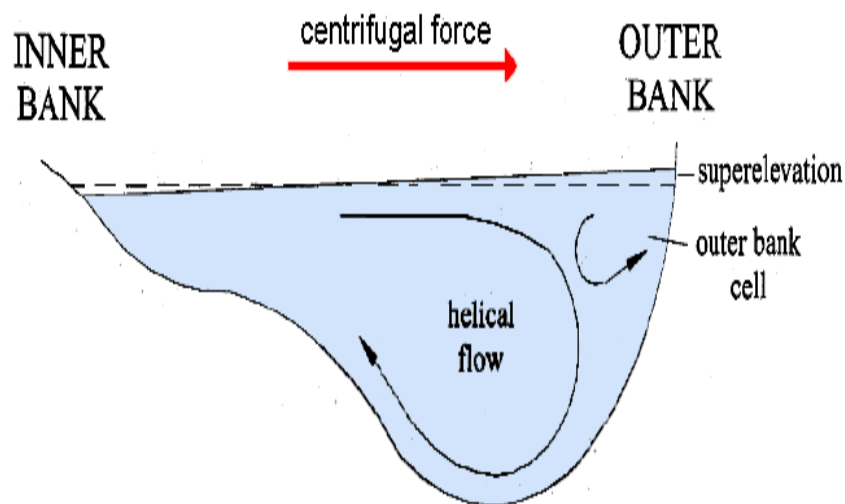


Figure-2. Secondary circulation and velocity in super elevation
Incurred channel (Camporeale. *et al*, 2007).

3. THE EXPERIMENTAL SETUP AND PROCEDURE

Experiments were conducted in the hydraulic laboratory of Building and Construction Engineering, UOT, Baghdad, Iraq, by using the sediment races flume which is rectangular in cross section and measures 60cm in width and 20cm in depth. The flume comprised three sections: the approach "straight reach" section 1.5m in length, 180°-bend working section, and a 2m straight section downstream connected at the end by a 40cm*60cm trap basin with an adjustable tailgate used to control flow depths. The bend section has the inner and outer radius of 37.5cm and 97.5cm, respectively, with arch length 3.06m. Figure-3 illustrates a plane sketch and Figure-4 shows the stage of preparation and maintenance, and after placing the sand races.

The base and sides of the channel are made of galvanized steel coated by using warming paint not affected by water corrosion as shown in Figure-4(a). A layer of uniform sand with 8.5 cm thickness and median diameter $d_{50} = 0.327\text{mm}$, and standard deviation $\sigma_g = 1.3$ was placed on the bed to cover the total length of the channel. The sand bed surface was levelled by a scraper. A point gauge was used to measure the water surface level and the topography of the channel bed after the completion of run and dewatering as shown in Figure-5(b). PVC pipes with 3, 4 and 6 cm diameter and 20cm height (to extend above water surface) are used to simulate the pier models. The larger diameter is selected to be in the context of the recommendation of [5] that it should not exceed 10% of flume width to ensure the side wall does not affect the scour value that formed around the pier. These models were installed at the centre of the flume at the desired



location within bend reach (working section). The parameter θ_p , which is equal to 0, 30, 60, 90, 120, 150 and 180 degrees, has been chosen to represent the location of the pier in the channel for 3cm diameter; however, the

other sizes of the pier model (i.e., 4cm and 6cm) are tested just at $\theta_p=90^\circ$. In all experiments, the same discharge equals to 218.559 l/min and the flow depth at the approach section was 2.8cm.

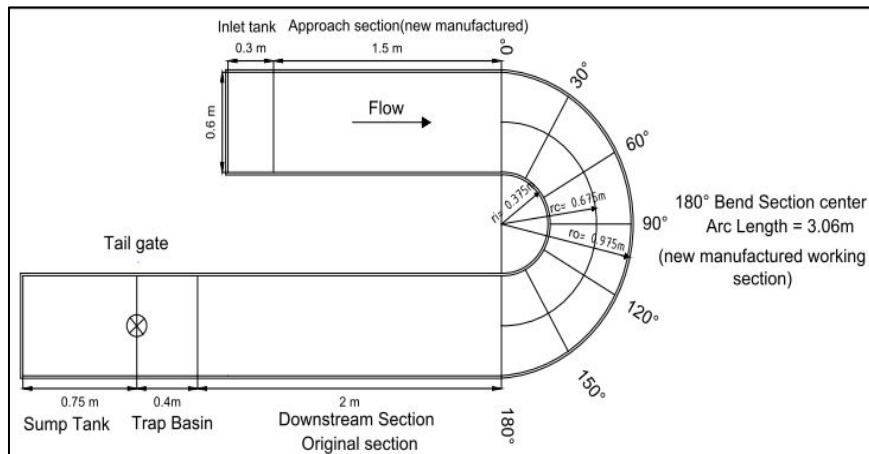


Figure-3. Plane sketch of flume sections with necessary dimensions (Al-Ibadi, 2016).



Figure-4. The flume at stage of preparation for experimental program; (a) without sediment (b) after put sand as a movable bed races.

4. FLOW CONDITION

The intensity of the flow in the experimental test should be suitable to satisfy the clear water flow condition at the approach section, whereas at the bend sections it helps to access the maximum scour in the outer bank and the local scour at the pier. Many attempts have been made which found the appropriate discharge and flow depths at the approach section to achieve this aim to be 218.56 l/min, and 2.8cm, respectively. Accordingly, the mean velocity at the threshold of the bed sediment motion (critical flow velocity) at the approach section (V_c) is 0.2172m/s. However, the mean flow velocity at the approach section (V) is 0.2168m/s. This velocity give a Froude number equal to 0.414, where this value of Froude number is consistent with the context of the flow usual in

the rivers. Therefore, the working intensity in all experiments undertaken is $V/V_c = 0.998$; such intensity ensures that the flow at the approach section is located within the clear water flow condition.

5. DURATION OF TEST

In order to find a more realistic equilibrium time, a 6cm -in -diameter pier was installed at the centre of flume first at the approach section, then a run was conducted for the periods 1, 2, 3, 3.5 and 4 hours. The scour depth at the nose of the pier has been measured by using point gauge at the end of each run after dewatering. However, the second position of the pier was at $\theta_p=90^\circ$ and the same procedure of runs and measurements are followed. For both tests, the scour depth was sharply



increased during the first 100 min of test after which the trend of scour increases became low and was approximated to be constant after 3.5 hours. It is noticed that 95% of the local scour was achieved at 3.5 hours for both locations. According to these results and for more accuracy, a four-hour period of the run was selected to be the equilibrium time and adopted for the experimental program undertaken.

6. RESULT ANALYSIS AND DISCUSSIONS

As mentioned previously, the single circular pier is installed at the centre of each 30° of 180° bend to show the effect of its location within bend reach on the amount of local scour. At the end of each run, the measurements have been taken both longitudinally and transversely for a bed which formed at and near the pier location. These measurements are recorded to represent the depth of scour

and deposition relative to a plain bed of sand races before the run. The main aim of this research is to find the modification factor due to bend (K_{bend}); this factor is calculated by dividing the scour depth which is formed at the nose of the pier when it is located at θ_p to the scour when the pier is located at straight reach. Figure-5 illustrates the symbols of the depths of bed form which are measured at equilibrium time (i.e., after 4 hours of run). In these figures, W_h is a maximum width of scour hole, L_h is a maximum length of scour hole, L_p is a maximum length of point bar, d_s is a maximum depth of scour hole at upstream face (nose) of pier, d_{so} is a maximum depth of scour hole from the outer bank, and d_{si} is a maximum depth of scour hole from the inner bank. All runs and measured parameters are listed in Table-1.

Table-1. Scour parameters for all experiments.

Run	Pier location (θ_p)	Pier diameter (cm)	d_s (mm)	d_{so} (mm)	d_{si} (mm)	L_h (cm)	L_p (cm)	W_h (cm)	K_{bend}
1	0	3	30	28	25	12	13	13.5	1
2	30	3	28.4	24.5	24.5	11	21.23	12	0.95
3	60	3	36	36	32	13.8	33.5	14	1.2
4	90	3	46	42	43	24.1	0	20	1.53
5	90	4	48	37	38.5	18.8	14.15	21	1.3
6	90	6	53	40	45	25.4	15.8	25	1.1
7	120	3	42	38	27	22.37	22.38	18.5	1.4
8	150	3	29	32	25	13.52	26.4	13	0.97
9	180	3	20	20	15	11.5	18	10	0.67

Figures 6 to 12 show a longitudinal profile of bed level along the bend reach when the pier is located first at $\theta_p = 0^\circ$ then at $\theta_p = 30^\circ$ and so on. In Figure-9, the longitudinal profiles for the three sizes of the pier are drawn to illustrate the variation in bed level due to the influence of pier diameter. The transverse bed levels across the center of the pier when it is installed at different positions in the bend are shown in Figure-13, while Figure-14 illustrates the variation of bed level transversely with pier size at $\theta_p = 90^\circ$. The modification factor (K_{bend}) seems to depend on the pier location within the bend; accordingly, its value is not constant. Figure-15 shows the trend of this factor with the sector angle and the radius of the bend. The best-fit formula of this factor at a determination coefficient $R^2 = 0.9876$ is

$$K_{bend} = 0.813 \left(\frac{\theta_p \pi r}{180} \right)^4 - 3.795 \left(\frac{\theta_p \pi r}{180} \right)^3 + 5.083 \left(\frac{\theta_p \pi r}{180} \right)^2 - 1.63 \left(\frac{\theta_p \pi r}{180} \right) + 1.009(1)$$

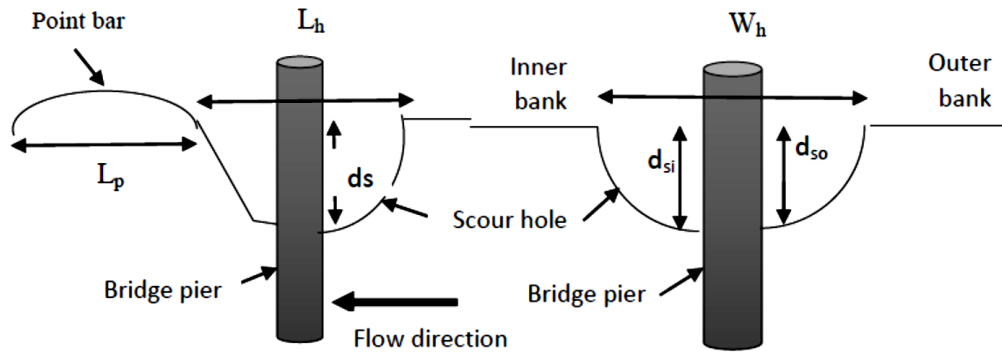
The variation of length L_h and width W_h of scour hole with the location of the pier are illustrated in Figure-16. It is evident that the length of the scour hole slightly

decreases when the pier is located within the first one-third of the bend; then it begins to increase continuously within the second third of the bend after which it tends again to decrease when the pier is located within the final third of the bend. The longest hole as clearly shown by the trend line was at $\theta_p \approx 110^\circ$. In terms of width, the same trend as for length is observed; however, the increase in the sector was less severe compared to the state of the length. Also, the trend lines show that the length of the scour hole is nearly equal to or in fact slightly less than the width of the hole when the pier is located within the first one-third and near the end of the last third, while the reverse result occurs within the second third besides, the difference seems more exaggerated. Figure-17 shows the variations of maximum depth of scour hole due to changes of pier location within the bend reach. The trend of variations of the depth of scour is same as for length and width of the scour hole. According to data points, the maximum values of scour depth is recorded when the pier is installed at section 90° , whereas the polynomial best-fit trend line for data points show that the maximum scour may occur practically if the pier is located at $\theta_p = 100^\circ$. The size of the pier has also been tested to show its effect on the scour



amount and feature, where three different diameter single piers are installed individually at $\theta_p=90^\circ$. From Figure-18 it can be deduced that the increase in the size of pier leads to a steady increase in the width of the scour hole. However, the length of the scour hole decreases at the first step of the increase in pier size and then starts to increase.

As has been emphasized in all relevant literature, that when the pier is located in a straight reach the larger diameter leads to a larger local scour at the nose of the pier for the same flow conditions. This case also have been noted when the piers presence within the bend reach as shown in Figure-19.



a) Longitudinal profile of scour hole and point bar b) Transverse section of the scour hole

Figure-5. Schematic view of scour and deposition around pier longitudinally and transversely.

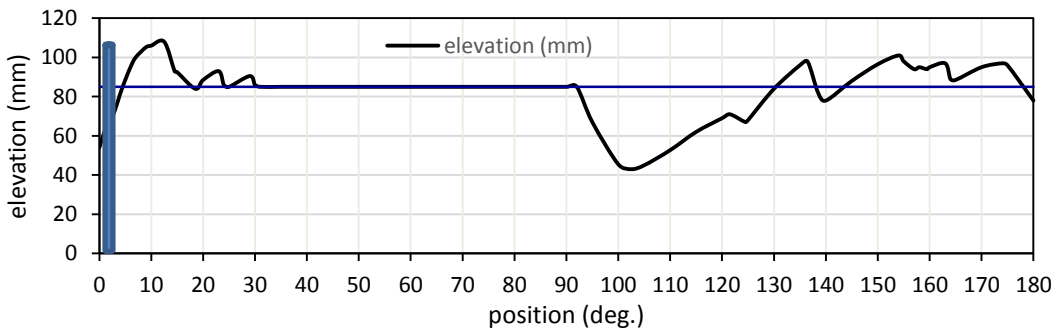


Figure-6. Longitudinal profile along the centreline of bend reach illustrates the bed elevations at equilibrium time when pier located at $\theta_p=0^\circ$ (beginning of bend).

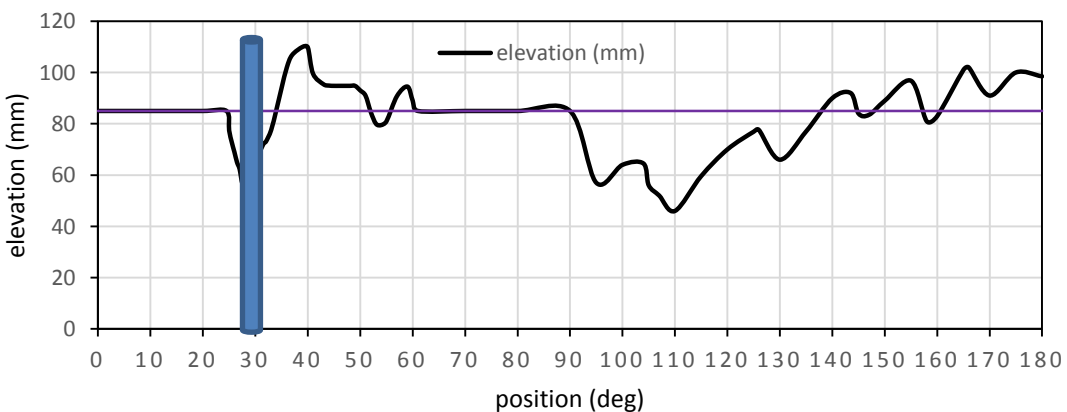


Figure-7. Longitudinal profile along the centreline of bend reach illustrates the bed elevations at equilibrium time when pier located at $\theta_p=30^\circ$.

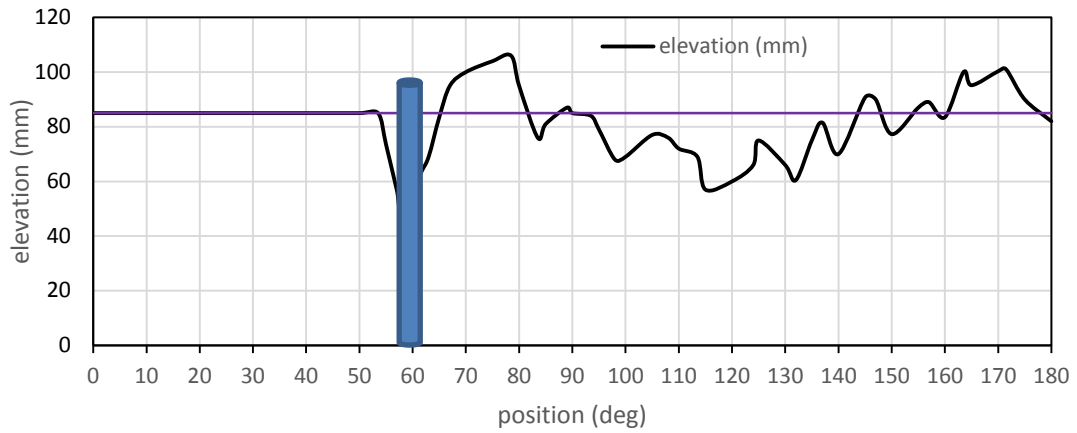


Figure-8. Longitudinal profile along the centreline of bend reach illustrates the bed elevations at equilibrium time when pier located at $\theta_p=60^\circ$.

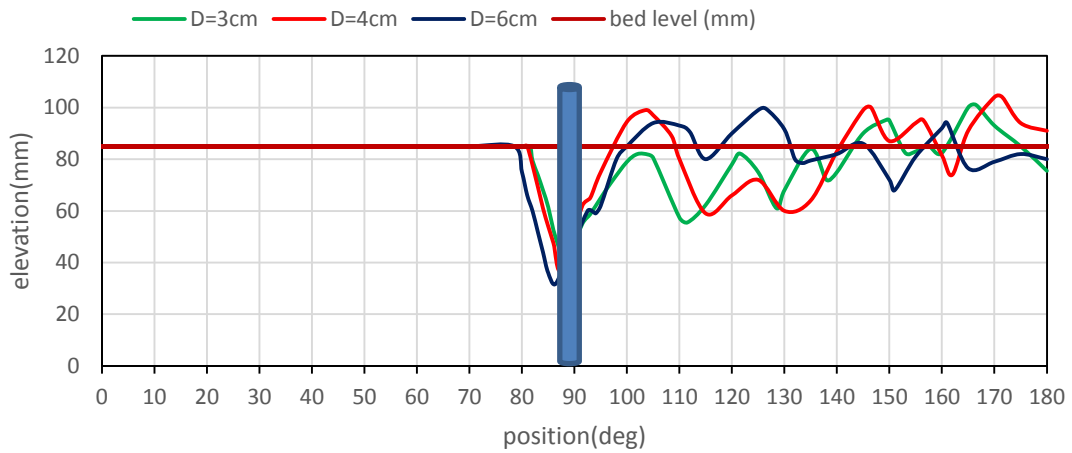


Figure-9. Longitudinal profile along the centreline of bend reach illustrates the bed elevations at equilibrium time when pier located at $\theta_p=90^\circ$ for different diameter.

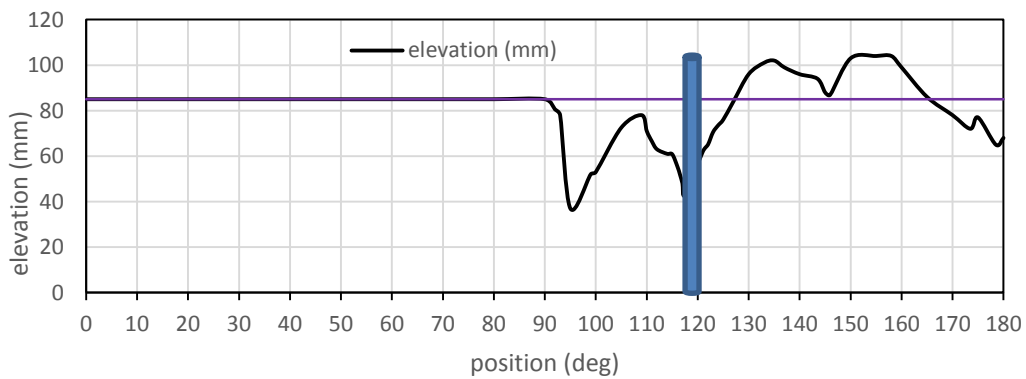


Figure-10. Longitudinal profile along the centreline of bend reach illustrates the bed elevations at equilibrium time when pier located at $\theta_p=120^\circ$.

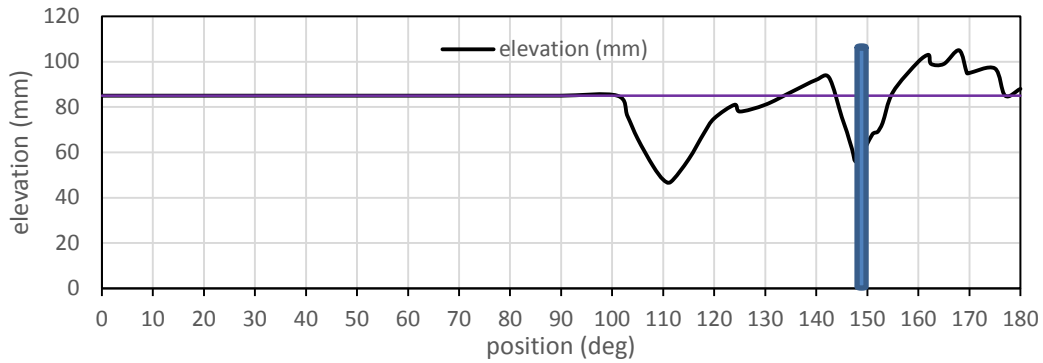


Figure-11. Longitudinal profile along the centreline of bend reach illustrates the bed elevations at equilibrium time when pier located at $\theta_p=150^\circ$.

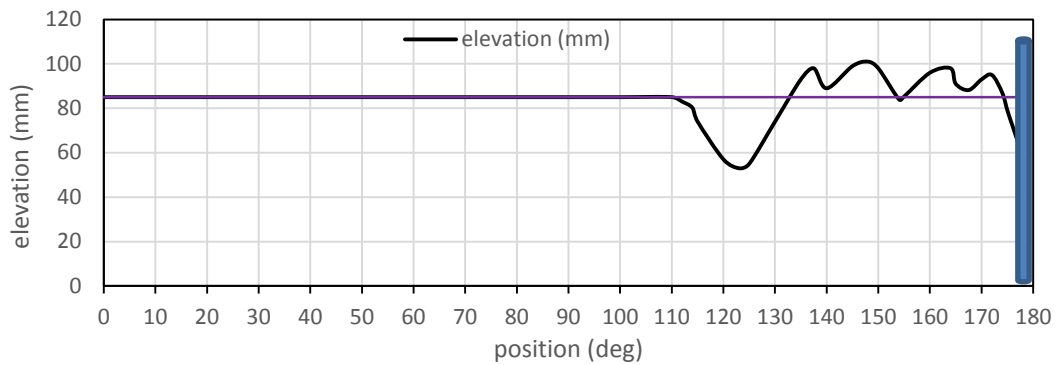


Figure-12. Longitudinal profile along the centreline of bend reach illustrates the bed elevations at equilibrium time when pier located at $\theta_p=180^\circ$.

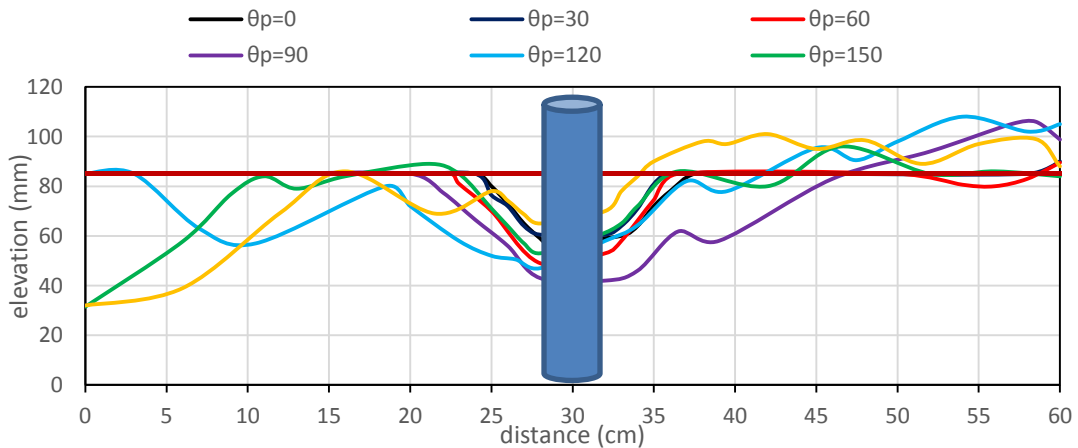


Figure-13. Transverse bed form elevation across the centre of pier for all pier positions.

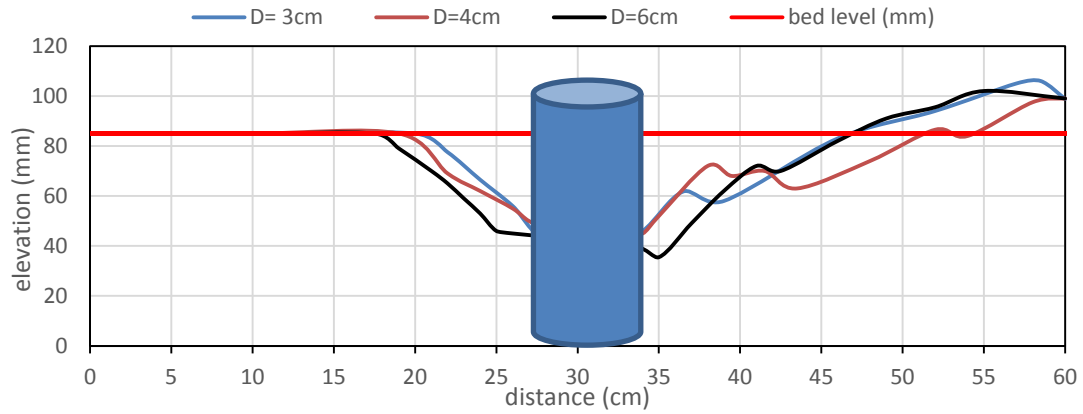


Figure-14. Transverse bed form elevation across the centre of pier at 90 degree for different diameter.

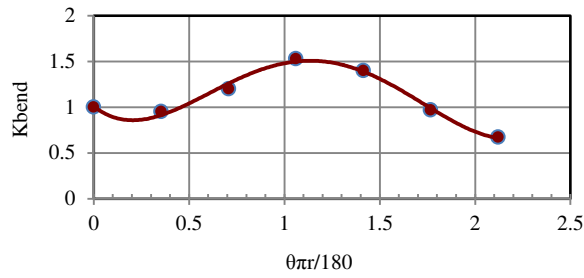


Figure-15. Modification Factor variation with location of Pier within bend.

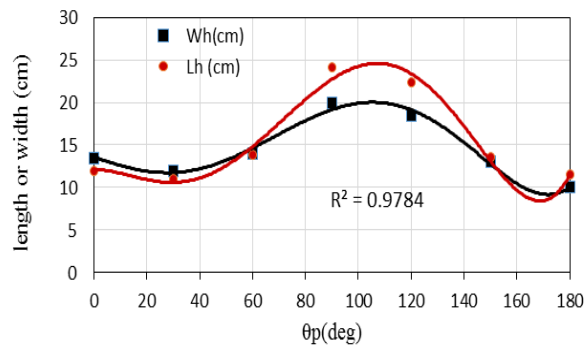


Figure-16. Length and Width of scour hole at different locations.

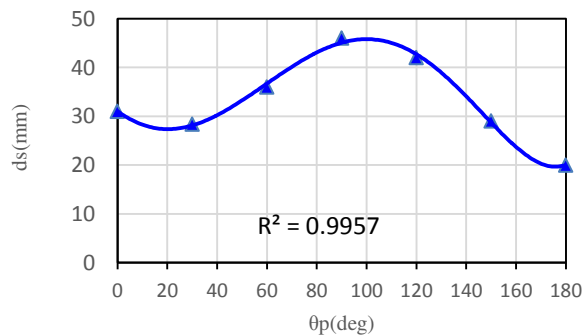


Figure-17. Maximum depth of scour hole at different locations.

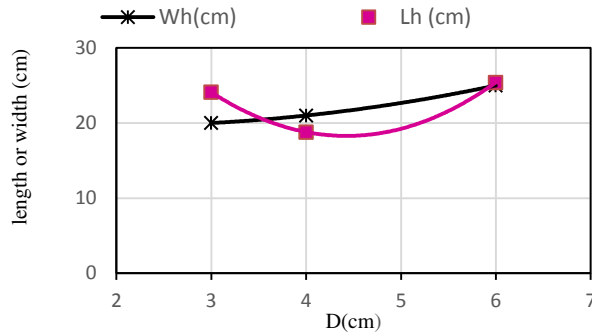


Figure-18. Effect of Pier size on Scour feature.

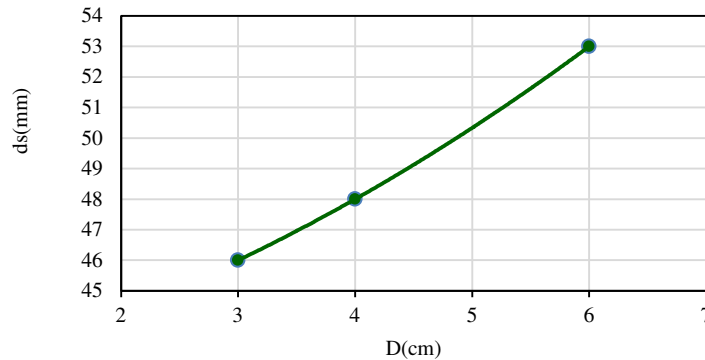


Figure-19. Effect of Pier size on maximum Scour depth.

7. CONCLUSIONS

This paper investigates the effects of bend reach on local scour which is formed around circular bridge piers when it is installed at the center line of any sector within a bend for clear water condition at the approach of straight reach. After collecting and analyzing the experimental data, the following conclusions are drawn from this experimental study. The maximum depth of scour hole d_s , maximum length L_h , and the maximum width W_h are recorded when a 3cm pier diameter is installed at $\theta_p=90^\circ$. Also, with the same context of straight reach, the scour increases with an increase the size of the pier for the same flow conditions. Finally, this study has provided the modification factor due to the presence of the pier within a bend. This factor can be used as a multiplication factor with any known equations proposed by researchers, which are basically derived to use for local scour calculations around piers located within straight reach (e.g., [2]; [10] and others). Through the results of the present work, the use of this factor has become necessary to take into account the effect of bend reach on local scour process.

Notation

The following symbols are used in this paper
 d_{50} = mean particle size of sand
 σ_g = standard deviation
 θ_p = location of the pier in the channel

V_c = the mean velocity at threshold of motion of bed sediment for approach flow
 V = the mean velocity at approach flow
 D = pier diameter
 W_h = maximum width of scour hole
 L_h = maximum length of scour hole
 L_p = maximum length of point bar,
 d_s = maximum depth of scour hole at upstream face of pier
 d_{s_o} = maximum depth of scour hole from outer bank side
 d_{s_i} = maximum depth of scour hole from inner bank side.
 K_{bend} = Modification factor due to bend
 θ_p = the angle of sector at pier location

REFERENCES

[1] Al-Ibadi, B. A. 2016. Performance of different configurations of submerged vanes as a river training structure aloes 180° bend. A thesis submitted to the Building and Construction Department, University of Technology, Iraq.
 [2] Breusers H.N.C., Nicollet G., and Shen H.W. 1977. Local scour around cylindrical piers. Journal of Hydraulic Research 15:3, 211-252, DOI:10.1080/00221687709499645.



- [3] Breusers H.N.C. and Raudkivi A.J. 1991. Scouring, Hydraulic Structure Design Manual. No.2, IAHR, Balkema. p. 143.
- [4] Camporeale C., Perona P., Porporat, A. and Ridolfi L. 2007. Hierarchy of models for meandering rivers and related morph dynamic processes, Reviews of Geophysics. 45, RG1001, DOI:10.1029/2005RG000185.
- [5] Chiew Y. M., Melville B.W. 1987. Local Scour around Bridge Piers. Journal of Hydraulic Research. 25(1): 15-26.
- [6] Gamal Elsaed, Hossam Elersawy, Mohammad Ibraheem, Fatma Samir. 2015. Bridge Pier Scour Evaluation in Meandering Channels. Journal of International Association of Advanced Technology and Science (JIAATS). 16(9): 1-12.
- [7] Gottlieb L. 1976. Three-Dimensional Flow Pattern and Bed Topography in Meandering Channels Series Paper 11, Institute of Hydrodynamics, Engineering Technology University, Denmark.
- [8] Jueyi Sui, Daxian F., and Bryan W. Karney. 2006. An experimental Study into Local Scour in a Channel Caused by a 90° bend. Canadian Journal of Civil Engineering 33: DOI:101139/L06-037, pp. 902-911.
- [9] Masjedi A., Bejestan M. S., and Esfandi A. 2010. Reduction of Local Scour at a Bridge Pier fitted with a Collar in a 180 degree Flume Bend (case study: Oblong Pier). 9th International Conference on Hydrodynamics, October 11-15, Shanghai-China, DOI: 10.1016/S1001-6058(10) 60012-1, pp.646-650.
- [10] Melville B.W. and Sutherland A.J. 1988. Design method for local scour at bridge piers. Journal of Hydraulic Engineering, ASCE, 114:10, 1210-1226.
- [11] Odgaard J. and Bergs A. 1988. Flow Process in a Curved Alluvial Channel. Water Resources Research. 24(1): 45-56.
- [12] Peter K. K. and John F. K. 1984. Secondary Current and River-Meander Formation. Journal of Fluid Mechanics. 144(1): 217-229.
- [13] Richardson E.V and Davis S.R. Evaluating Scour at bridge (4th ed.) 2001. Federal Highway Administration. Hydraulic Engineering Circular No.18. FHWA NHI 01-001.
- [14] Won S. and Young J. J. 2010. Velocity Distribution of Secondary Currents in Curved Channels. Science Direct. 22(5): 617-622.
- [15] Yaser E., Amin S. Salamatian and Masoud G. 2008. Scour at cylindrical bridge pier in 180 degree channel bend. Fourth International Conference on Scour and Erosion.